GaN electronics for high power, high temperature applications

S.J. Pearton [a],*, F. Ren [b], A.P. Zhang [b], G. Dang [b], X.A. Cao [a], K.P. Lee [a], H. Cho [c],
B.P. Gila [a], J.W. Johnson [b], C. Monier [a], C.R. Abernathy [a], J. Han [d], A.G. Baca [d],
J.-I. Chyi [e], C.-M. Lee [e], T.-E. Nee [e], C.-C. Chuo [f], S.N.G. Chu [g]

[a] *Department of Materials Science and Engineering, University of Florida, 100 Rhines Hall, PO Box 116400, Gainesville, FL 32611-64600, USA*
[b] *Department of Chemical Engineering, University of Florida, Gainesville, FL 32611, USA*
[c] *Department of Materials Engineering, Miryang National University, Kyungnam, South Korea*
[d] *Sandia National Laboratories, Albuquerque, NM 87185, USA*
[e] *Department of Electrical Engineering, National Central University, Chung-Li, 32054, Taiwan*
[f] *Department of Physics, National Central University, Chung-Li, 32054, Taiwan*
[g] *Bell Laboratories, Lucent Technologies, Murray Hill, NJ 07974, USA*

Abstract

A brief review is given of recent progress in fabrication of high voltage GaN and AlGaN rectifiers, GaN/AlGaN heterojunction bipolar transistors and GaN metal-oxide semiconductor field effect transistors. Improvements in epitaxial layer quality and in fabrication techniques have led to significant advances in device performance. © 2001 Elsevier Science B.V. All rights reserved.

Keywords: GaN; Rectifiers; Bipolar transistors; MOSFETs.

1. Introduction

1.1. Symposium: C, session: # V111, unique reference number: C-V111-1

There are also numerous advantages of the AlGaInN system for high power electronics, including wide bandgaps for high voltage and temperature operation, good transport properties, the availability of heterostructures and finally the experience base accumulated during the development of nitride-based light-emitting diodes and lasers. Most of the work on nitride-based electronics has focused on AlGaN/GaN high electron mobility transistors for power microwave applications [1–6], but there are potential advantages to the use of bipolar transistors (either heterojunction bipolar transistors or bipolar junction transistors) in some applications because of their higher current densities, better linearity and more uniform threshold voltages. GaN/AlGaN bipolar transistors are an attractive option for various satellite, radar and communica-

tions applications in the 1–5 GHz frequency range, at temperatures > 400°C and powers > 100 W. Traditional Si-based technologies cannot support such requirements, but the wide bandgap GaN materials system is capable of reaching this performance level. A summary of progress in GaN electronics is given in Table 1

In addition there is a strong interest in developing high current, high voltage switches in the AlGaN materials system for applications in the transmission and distribution of electric power and in the electrical subsystems of emerging vehicle, ship and aircraft technology. It is expected that packaged switches made from AlGaN may operate at temperatures in excess of 250°C without liquid cooling, thereby reducing system complexity, weight and cost. In terms of voltage requirements, there is a strong need for power quality enhancement in the 13.8 kV class, while it is estimated that availability of 20–25 kV switches in a single unit would cause a sharp drop in the cost of power flow control circuits. Schottky and $p-i-n$ rectifiers are an attractive vehicle for demonstrating the high voltage performance of different materials systems and blocking voltages from 3–5.9 kV have been reported in SiC devices. The reverse leakage current in Schottky rec-

* Corresponding author. Tel.: + 1-352-8461181; fax: + 1-352-8461182.

E-mail address: spear@mse.ufl.edu (S.J. Pearton).

tifiers is generally far higher than expected from thermionic emission, most likely due to defect states

Table 1
Historical development of GaN-based electronics

Year	Event	Authors
1969	GaN by hydride vapor phase epitaxy	Maruska and Tietjen
1971	MIS LEDs	Pankove et al.
	GaN by MOCVD	Manasevit et al.
1974	GaN by MBE	Akasaki and Hayashi
1983	AlN intermediate layer by MBE	Yoshida et al.
1986	Specular films using AlN buffer	Amano et al.
1989	p-type Mg-doped GaN by LEEBI and GaN p–n junction LED	Amano et al.
1991	GaN buffer layer by MOCVD	Nakamura
1992	Mg activation by thermal annealing	Nakamura et al.
	AlGaN/GaN two-dimensional electron gas	Khan et al.
1993	GaN MESFET	Khan et al.
	AlGaN/GaN HEMT	Khan et al.
	Theoretical prediction of piezoelectric effect in AlGaN/GaN	Bykhovski et al.
1994	InGaN/AlGaN DH blue LEDs (1 cd)	Nakamura et al.
	Microwave GaN MESFET	Binari et al.
	Microwave HFET, MISFET	Binari et al.; Khan et al.
	GaN/SiC HBT	Pankove et al.
1995	AlGaN/GaN HEMT by MBE	Ozgur et al.
1996	Doped channel AlGaN/GaN HEMT	Khan et al.
	Ion-implanted GaN JFET	Zolper et al.
	340 V V_{GD} AlGaN/GaN HEMT	Wu et al.
	1st blue laser diode	Nakamura and Fosal
1997	Quantification of piezoelectric effect	Asbeck et al.
	AlGaN/GaN HEMT on SiC	Binari et al.; Ping et al.; Gaska et al.
	1.4 W @ 4 GHz	Thibeault et al.
	0.85 W @ 10 GHz	Siram et al.
	3.1 W mm^{-1} at 18 GHz	Wu et al.
1998	3.3 W	Sullivan et al.
	p/n junction in LEO GaN	Kozodoy et al.
	HEMT in LEO GaN	Mishra et al.
	6.8 W mm^{-1} (4 W) @ 10 GHz HEMT on SiC	Sheppard et al.
	10^{-4} Hooge factor for HEMT on SiC	Levinshtein et al.
	1st AlGaN/GaN HBT	McCarthy et al.; Ren et al.
	1st GaN MOSFET	Ren et al.
1999	9.1 W mm^{-1} @ 10 GHz HEMT on SiC	Mishra et al.
	GaN BJT (npn)	Yoshida et al.
2000	4.3 kV AlGaN rectifier	Zhang et al.
	pnp GaN/AlGaN HBT	Zhang et al.
	pnp GaN BJT	Zhang et al.

around the contact periphery. To reduce this leakage current and prevent breakdown by surface flash-over, edge termination techniques such as guard rings, field plates, beveling or surface ion implantation are necessary. However in the few GaN rectifiers reported so far, there has been little effort on employing edge termination methods and no investigation of the effect of increasing the bandgap by use of AlGaN.

In this paper we will detail recent results in GaN power electronic devices, including Schottky rectifiers, HBTs, BJTs, MOSFETs and HEMTs. The pace of advancement of these technologies has been remarkably rapid in the past 2 years.

2. GaN Rectifiers

For these devices, the GaN was grown on c-plane Al$_2$O$_3$ substrates by Metal Organic Chemical Vapor Deposition using trimethylgallium and ammonia as the precursors. For vertically-depleting devices, the structure consisted of a 1 μm n^+ (3×10^{18} cm^{-3}, Si-doped) contact layer, followed by undoped ($n = 2.5 \times 10^{16}$ cm^{-3}) blocking layers which ranged from 3–11 μm thick. These samples were formed into mesa diodes using Inductively Coupled Plasma etching with Cl$_2$/Ar discharges (300 W source power, 40 W rf chuck power). The dc self-bias during etching was -85 V. To remove residual dry etch damage, the samples were annealed under N$_2$ at 800°C for 30 s. Ohmic contacts were formed by lift-off of e-beam evaporated Ti/Al, annealed at 700°C for 30 s under N$_2$ to minimize the contact resistance. Finally, the rectifying contacts were formed by lift-off of e-beam evaporated Pt/Au. Contact diameters of 60–1100 μm were examined.

For laterally-depleting devices, the structure consisted of ~ 3 μm of resistive (10^7 ohms per square) GaN. To form ohmic contacts, Si$^+$ was implanted at 5×10^{14} cm^{-2}, 50 keV into the contact region and activated by annealing at 150°C for 10 s under N$_2$. The resulting n-type carrier concentration was 1×10^{19} cm^{-3}. The ohmic and rectifying contact metallization was the same as described above.

Three different edge termination techniques were investigated for the planar diodes:

1. use of a p-guard ring formed by Mg$^+$ implantation at the edge of the Schottky barrier metal. In these diodes the rectifying contact diameter was held constant at 124 μm, while the distance of the edge of this contact from the edge of the ohmic contact was 30 μm in all cases.

1. use of p-floating field rings of width 5 μm to extend the depletion boundary along the surface of the SiO$_2$ dielectric, which reduces the electric field
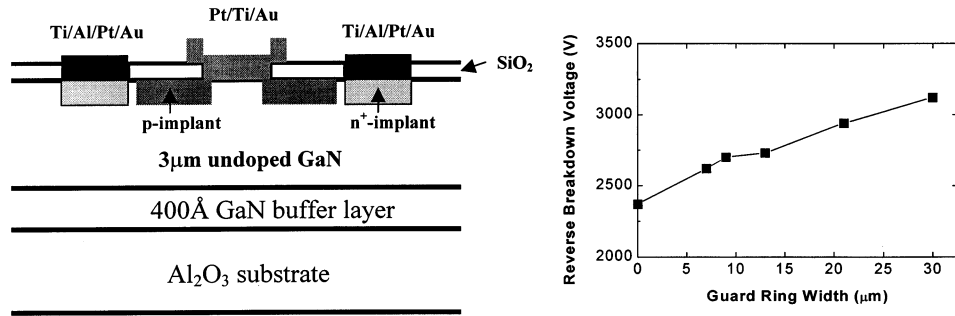
Fig. 1. (left) View of rectifiers with p-type guard. (right) Variation of V_B with guard ring width.

crowding at the edge of this boundary. In these structures a 10 μm wide p-guard ring was used, and 1–3 floating field rings employed.

1. use of junction barrier controlled Schottky (JBS) rectifiers, i.e. a Schottky rectifier structure with a p–n junction grid integrated into its drift region.

In all of the edge-terminated devices the Schottky barrier metal was extended over an oxide layer at the edge to further minimize the field crowding, and the guard and field rings formed by Mg^+ implantation and 1100°C annealing.

Fig. 1 (left) shows a schematic of the planar diodes fabricated with the p-guard rings, while the right of the Figure shows the influence of guard ring width on V_B at 25°C. Without any edge termination, V_B is ~ 2300 V for these diodes. The forward turn-on voltage was in the range 15–50 V, with a best on-resistance of 0.8 Ω m². The figure-of-merit $(V_B)^2/R_{ON}$ was 6.8 MW cm^{-2}. As the guard-ring width was increased, we observed a monotonic increase in V_B, reaching a value of ~ 3100 V for 30 μm wide rings. The figure-of-merit was 15.5 MW cm^{-2} under these conditions. The reverse leakage current of the diodes was still in the nA range at voltages up to 90% of the breakdown value. Similar results were obtained with the field rings or JBS control.

The results shown in Fig. 1 are convincing evidence that proper design and implementation of edge termination methods can significantly increase reverse breakdown voltage in GaN diode rectifiers and will play an important role in applications at the very highest power levels. For example, the target goals for devices intended to be used for transmission and distribution of electric power or in single-pulse switching in the subsystem of hybrid-electric contact vehicles are 25 kV standoff voltage, 2 kA conducting current and forward voltage drop $< 2\%$ of the standoff voltage. At these power levels, it is expected that edge termination techniques will be essential for reproducible operation.

To place our results in context with reported SiC Schottky diode performance reported in literature, Fig. 2 shows a plot of specific on-resistance versus reverse

breakdown voltage for SiC and GaN diodes, together with the calculated (theoretical) performance. The 3.1 kV result for GaN reported here is still well below the theoretical value, indicating that further improvement in processing and materials are needed. Some reported SiC devices have performance close to the theoretical limit, reflecting greater maturity of this technology at present.

3. AlGaN rectifiers

The undoped $Al_xGa_{1-x}N$ layers were grown by atmospheric pressure Metal Organic Chemical Vapor Deposition at 1040°C (pure GaN) or 1100°C (AlGaN) on (0001) oriented sapphire substrates. The precursors were trimethylgallium, trimethlygaluminum and ammonia, with H_2 used as a carrier gas. The growth was performed on either GaN (in the case of GaN active layers) or AlN (in the case of AlGaN active layers) low temperature buffers with nominal thickness of 200 Å. The active layer thickness was ~ 2.5 μm in all cases and the resistivity of these films was of order 10^7 Ω cm.
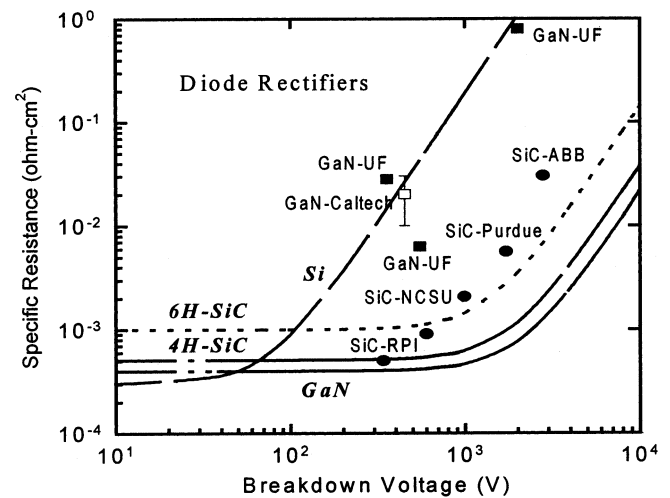

Fig. 2. On-resistance versus blocking voltage for SiC and GaN diode rectifiers. The performance limits and GaN devices are shown by the solid lines.
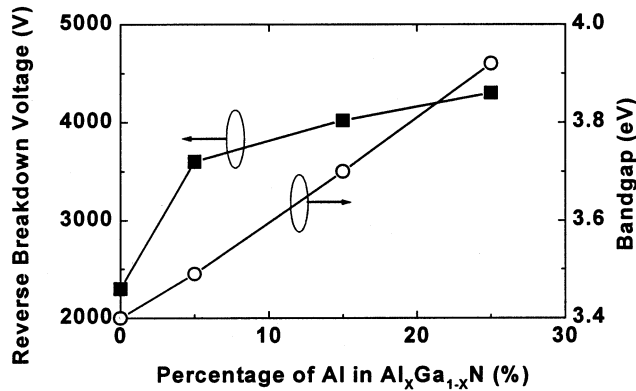
Fig. 3. Variation of V_{RB} in $Al_xGa_{1-x}N$ rectifiers without edge termination, as a junction of Al concentration. The bandgaps for the AlGaN alloys are also shown.

To form ohmic contacts in some cases, Si^+ was implanted at 5×10^{14} cm^{-2}, 50 keV into the contact region and activated by annealing at 1150°C for 10 s under N_2. The contacts were then formed by lift-off of *e*-beam evaporated Ti/Al/Pt/Au annealed at 700°C for 30 s under N_2. The rectifying contacts were formed by lift-off of *e*-beam evaporated Pt/Ti/Au (diameter 60–1100 μm). The on-resistance of the AlGaN diodes was higher than for pure GaN, due to higher ohmic contact resistance. The lowest R_{ON} achieved was 3.2 Ω cm^2, leading to a figure-of-merit of ~ 5.5 MW cm^{-2}.

Fig. 3 shows the variation of V_{RB} with Al percentage in the AlGaN active layers of the rectifiers. In this case we are using the V_{RB} values from diodes without any edge termination or surface passivation. The calculated bandgaps as a function of Al composition are also shown, and were obtained from the relation

$$Eg(x) = EgGaN(1 - x) + EgAlN \cdot x - bx(1 - x),$$

where x is the AlN mole fraction and b is the bowing parameter with value 0.96 eV. Note that V_{RB} does not increase in linear fashion with bandgap. In a simple theory V_{RB} should increase as $(Eg)^{1.5}$, but it has been empirically established that factors such as impact ionization coefficients and other transport parameters need to be considered and that consideration of Eg alone is not sufficient to explain measured V_{RB} behavior. The fact the V_{RB} increases less rapidly with Eg at higher AlN mole fractions may indicate increasing concentrations of defects that influence the critical field for breakdown.

The reverse *I–V* characteristics of all of the rectifiers showed $I \propto V^{0.5}$ over a broad range of voltage (50–2000 V), indicating that Shockley–Read–Hall recombination is the dominant transport mechanism. The current density in all devices was in the range $5–10 \times 10^{-6}$ A cm^{-2} at 2 kV. At low biases (≤ 25 V) the reverse current was proportional to the perimeter of the rectifying contact, suggesting that surface contributions

are the most important in this voltage range. For higher biases, the current was proportional to the area of the rectifying contact. Under these conditions, the main contribution to the reverse current is from under this contact, i.e. from the bulk of the material. It is likely that the high defect density in heteroepitaxial GaN is a primary cause of this current.

When pushed beyond breakdown, the diodes invariably failed at the edges of the rectifying contact. As described earlier, the use of metal field plate contact geometries with SiO_2 as the insulator and either guard rings or floating field rings significantly increased V_B. These rectifiers generally did not suffer irreversible damage to the contact upon reaching breakdown and could be re-measured many times.

4. GaN/AlGaN heterojunction bipolar transistors

Both *npn* and *pnp* HBTs have been fabricated with emitter contact diameters in the range 50–100 μm. HBT power microwave amplifiers are mostly designed on common-emitter or common-base operation. The current gain is greater than unity only in the common-emitter mode, but the common-base mode is attractive because of the possibility of appreciable power gain obtained through the impedance transformation offered by this amplifier.

In all of our devices we have observed that the saturated collector current was nearly equal to the emitter current, which indicates high emitter injection efficiency. Gummel plots showed dc current gains of 15–20 at room temperature. In many of the devices it is difficult to obtain common-emitter operation due to leakage in the collector-base junction, and at all temperatures (25–300°C) the junction ideality factors for both emitter-base and collector base junctions were close to two, indicative of significant recombination. By removing the base contact we observed no collector current, which confirms the transistor modulation.

For *npn* devices the performance is limited by the high base resistance, which originates from the deep ionization level of the Mg acceptors. In these devices we have achieved maximum current densities of 2.55 kA cm^{-2} at $V_{BC} = 8$ V, corresponding to power densities of 20.4 kW cm^{-2}.

There are two advantages to the *pnp* configuration for AlGaN/GaN HBTs. Firstly, there is a large emitter-base energy bandgap offset than in *npn* structures, and secondly, the base resistance will be much lower due to higher doping level achievable in *n*-type material. The best *pnp* HBTs we fabricated can be operated up to current densities of over 2 kA cm^{-2} at 25 V, corresponding to power densities above 50 kW cm^{-2}. A Gummel plot is shown in Fig. 4.
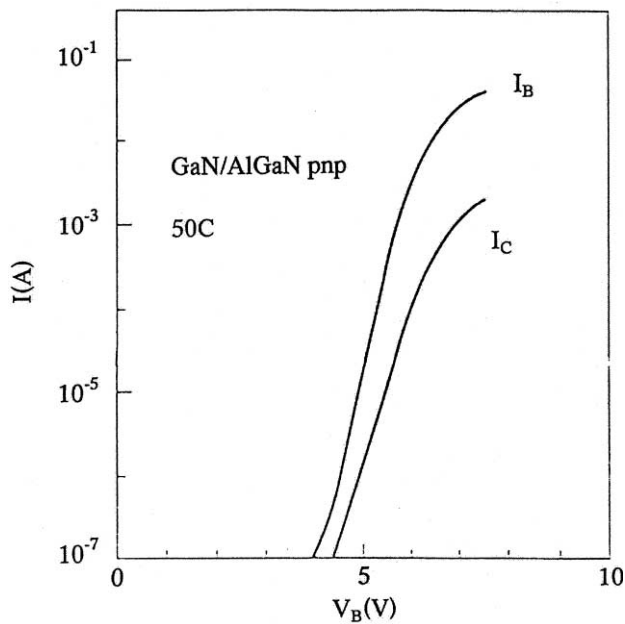
Fig. 4. Gummel plot of *pnp* HBT with $V_{CB} = 0$.

5. GaN bipolar junction transistors

The epitaxial growth of BJTs is simpler than for HBTs because the emitter layer is comprised of GaN rather than AlGaN. In our *npn* devices we have achieved maximum current densities of 3.6 kA cm^{-2} at a collector-base voltage of 15 V, corresponding to a power density of 54 kW cm^{-2}. The maximum common-emitter dc current gain was ~ 15 for temperatures up to 300°C. The operation of both GaN BJTs and GaN/AlGaN HBTs was simulated using a program based on the drift-diffusion model. This simulation showed that at low current densities the HBT enjoys and advantage due to the conduction band offset, but that at higher current densities the results converged. This suggests that simple BJTs are useful as power devices.

The dc characteristics were measured up to a V_{BC} of 65 V in the common-base mode. A stable current density of 204 A cm^{-2} was run at this voltage, corresponding to a power density of 40 kW cm^{-2}. These values can clearly be increased by optimized design of the layer structure and mask layout. The devices showed little fall-off in performance at temperatures up to 250°C.

6. GaN metal oxide semiconductor field effect transistors

A GaN depletion-mode metal oxide semiconductor field effect transistor was demonstrated, using $Ga_2O_3(Gd_2O_3)$ as the gate dielectric, similar to the approach reported for GaAs and InGaAs. The MOS gate reverse breakdown voltage was > 35 V, significantly higher than obtained using a simple Pt Schottky gate on the same material. A maximum extrinsic transconductance of 15 mS mm^{-1} was obtained at $V_{DS} = 30$ V and device performance was limited by the contact resistance. A unity current gain cut-off frequency, f_T, and maximum frequency of oscillation, f_{MAX}, of 3.1 and 10.3 GHz, respectively were measured at $V_{DS} = 25$ V and $V_{GS} = -20$ V. The device performance can be improved by optimizing the layer structure using a thin and heavily doped channel layer, which will reduce the contact resistance and enhance the transconductance.

7. Summary

Tremendous progress has been made in advancing the growth, processing and design of GaN power electronics in recent times. There are as yet no commercially-available devices and this may take another 3–5 years to occur.

Acknowledgements

References

[1] M.S. Shur, M.A. Khan, in: S.J. Pearton (Ed.), GaN and Related Materials II, Gordon and Breach, NY, 2000.

[2] S.C. Binari, L.B. Rowland, W. Kruppa, G. Kelner, K. Doverspike, D.K Gaskill, Electron. Lett. 30 (1994) 1248.

[3] L.F. Eastman, K.G. Chu, J. Smart, J.R. Shealy, Mat. Res. Soc. Symp. Proc. 512 (1998) 3.

[4] S.T. Sheppard, K. Doverspike, W.L. Pribble, S.T. Allen and J.W. Palmour, 56th Device Research Conference, Charlottesville, VA, June 1998.

[5] Y.-F. Wu, B.J. Thibeault, B.P. Keller, S. Keller, S.P. DenBaars, U.K. Mishra, Topical Workshop on Heterostructure Electronics, Kanagawa, Japan, 1998.

[6] L. Daumiller, L. Kirchner, M. Kamp, K.J. Eheling, L. Pond, C.E. Weitzel and E. Kohn, 56th Device Research Conference, Charlottesville, CA, June 1998